Evaluation of Electromagnetic Fields produced by Overhead Transmission Lines

Jorge F.G. Casaca

***Abstract* - In this work, a method for the evaluation of 50Hz electromagnetic fields produced by overhead power lines is presented. This method allows for a correct evaluation of all voltages and currents in the system, including the currents in the subconductors of each phase bundle, the currents in the ground wires and the currents in the mitigation loop (if present). In the magnetic field calculation, the non-uniform character of the trajectory described by the conductors between towers, drawing a catenary, is considered. Using this method, a program for the calculation of magnetic and electric fields was produced. It can handle any line geometry, including the presence of a mitigation loop.**

I. INTRODUCTION

Due to the recent concerns that electromagnetic fields generated by overhead power lines might affect human health, namely to increase the risk of cancer, scientific community have been trying to find solutions that will reduce fields surrounding power lines [CARST95]. A lot of work has been conducted in recent years to develop instrumentation to evaluate power system magnetic and electric fields [BRAND06]-[WASHI92].

The International Commission of Non Ionizing Radiation Protection (ICNIRP) have published new guidelines concerning occupational and public exposure to electric and magnetic fields. The recommendations are 500μT and 10kV/m in occupational exposure, and 100μT and 5kV/m in public exposure [ICNIRP98]. The most of the countries have adopted those guidelines, however, in some other countries (like the United States or Switzerland) different limitations were followed.

In what concerns to magnetic field mitigation, a lot of solutions have been proposed [BRAND06],[SHPER96],[CELO02], [MEMAR05]-[WALL93].

The solutions include the reconfiguration of line geometry; the installation of single or double loops near the phase conductors [SHPER96]; the consideration of series-capacitor schemes to improve field mitigation [WALL93]; the use of underground cables, etc.

In this work, a MATLAB program for magnetic and electric field calculation was created. The program was designed to deal with different line configurations based on the mitigation loop solution (short circuited or with capacitor compensation). For this, a model including the two subconductors partition of each phase bundle, the ground wires influence and the effect of the catenary described by the line conductors between towers was considered.

The most of the studies, dealing with power lines, doesn't make use of these considerations, neglecting the ground wires, replacing bundle phase-conductors with equivalent single conductors with a GMR, replacing the sagged conductors with average height horizontal conductors.

This paper is organized into five sections, the first of which is introductory. Section II describes the magnetic field evaluation developed in this work. The calculation method of electric field is presented in section III. In section IV the results obtained are presented and discussed. Section V is reserved to conclusions.

II. MAGNETIC FIELD EVALUATION

A correct analysis of the magnetic field begins with the determination of all system currents (phase subconductors, ground wires and mitigation loop conductors, if present) based on the prescribed phase conductor currents $\mathbf{I_P}$

$$\mathbf{I_P} = \begin{bmatrix} I_1 \\ I_2 \\ I_3 \end{bmatrix} \tag{1}$$

Initially, we will consider the frequency-domain transmission line matrix equation for nonuniform multiconductor transmission lines

$$\begin{cases} \dfrac{d\boldsymbol{I}}{dz} = -\boldsymbol{Y'V} \\ \dfrac{d\boldsymbol{V}}{dz} = -\boldsymbol{Z'I} \end{cases} \tag{2}$$

where $\boldsymbol{Z'}$ refer the per-unit-length series-impedance matrix and $\boldsymbol{Y'}$ the per-unit-length shunt-admittance.

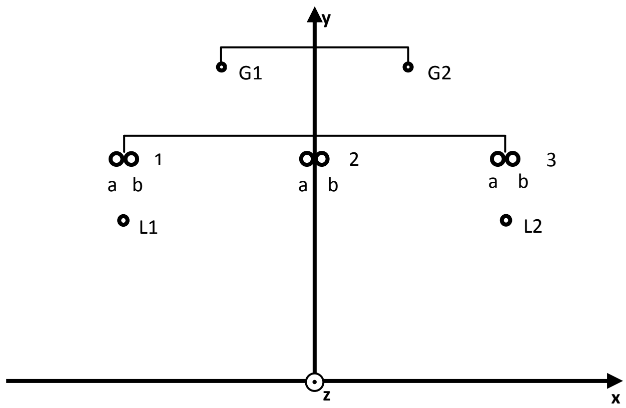

Figure 1 Cross section of a single circuit 400kV overhead power line

The matrices associated with all the currents and all the voltages of the line conductors are **I** and **V,** respectively.

$$\boldsymbol{V} = \begin{bmatrix} \boldsymbol{V}_1 \\ \boldsymbol{V}_2 \\ \boldsymbol{V}_3 \\ \boldsymbol{V}_G \\ \boldsymbol{V}_L \end{bmatrix}; \quad \boldsymbol{I} = \begin{bmatrix} \boldsymbol{I}_1 \\ \boldsymbol{I}_2 \\ \boldsymbol{I}_3 \\ \boldsymbol{I}_G \\ \boldsymbol{I}_L \end{bmatrix} \tag{3}$$

In (3) 1, 2 and 3 refer to the phase conductors, G refers to ground wires and L refers to the mitigation loop (figure 1). Unfolding the sub-matrices in (3) for the subconductors of each phase bundle, we obtain,

$$\boldsymbol{V}_1 = \begin{bmatrix} V_{1a} \\ V_{1b} \end{bmatrix}; \ \boldsymbol{V}_2 = \begin{bmatrix} V_{2a} \\ V_{2b} \end{bmatrix}; \ \boldsymbol{V}_3 = \begin{bmatrix} V_{3a} \\ V_{3b} \end{bmatrix};$$

$$\boldsymbol{V}_G = \begin{bmatrix} V_{G1} \\ V_{G2} \end{bmatrix}; \boldsymbol{V}_L = \begin{bmatrix} V_{L1} \\ V_{L2} \end{bmatrix}; \tag{4}$$

$$\boldsymbol{I}_1 = \begin{bmatrix} I_{1a} \\ I_{1b} \end{bmatrix}; \ \boldsymbol{I}_2 = \begin{bmatrix} I_{2a} \\ I_{2b} \end{bmatrix}; \ 3 = \begin{bmatrix} I_{3a} \\ I_{3b} \end{bmatrix};$$

$$\boldsymbol{I}_G = \begin{bmatrix} I_{G1} \\ I_{G2} \end{bmatrix}; \ \boldsymbol{I}_L = \begin{bmatrix} I_{L1} \\ I_{L2} \end{bmatrix}; \tag{5}$$

The per-unit-length series-impedance matrix is given by,

$$\boldsymbol{Z}'(\omega) = j\omega \boldsymbol{L_e} + \Delta \boldsymbol{Z_E}(\omega) + \Delta \boldsymbol{Z_{skin}}(\omega) \tag{6}$$

The matrix $\boldsymbol{L_e}$ is a frequency-independent real symmetric matrix which refers to the external-inductances. The entries of $\boldsymbol{L_e}$ are

$$\boldsymbol{L_{ii}} = \frac{\mu_0}{2\pi} ln \frac{2h_i}{r_i}; \ \boldsymbol{L}_{ki}|_{k\neq i} = \frac{\mu_0}{2\pi} ln \left[\frac{\sqrt{(h_i+h_k)^2+(x_i-x_k)^2}}{\sqrt{(h_i-h_k)^2+(x_i-x_k)^2}} \right] \tag{7}$$

Where r_i refers to the conductor radius, and h_i and x_i denote the vertical and horizontal coordinates of conductor i. $\boldsymbol{Z_E}$ represents the matrix of the earth impedance correction. This is a frequency dependent complex matrix that can be determined using Carson's functions or Dubanton's method (figure 2) [DUBAN69]. This is based on the method of images but where the plan of null potential is located at a complex depth $\bar{p}$ given by

$$\bar{p} = \frac{1}{\sqrt{j\omega\mu_0\sigma_t}} \tag{8}$$

where σ_t denotes the earth conductivity.

The matrix of the earth impedance correction $\boldsymbol{Z_E}$ is defined by

$$\Delta \boldsymbol{Z_E}(\omega) = \frac{j\omega\mu_0}{2\pi} ln \frac{\overline{D_{\iota k}}}{D_{ik}} \tag{9}$$

where $\overline{D_{\iota k}}$ is the complex distance between conductor k and the image of conductor I and D_{ik} is the same distance without the complex distance $\bar{p}$ to the ground. The matrix $\boldsymbol{Z_{skin}}$ is a frequency dependent complex diagonal matrix that can be determined through the skin-effect theory for cylindrical conductors [BRAND06].

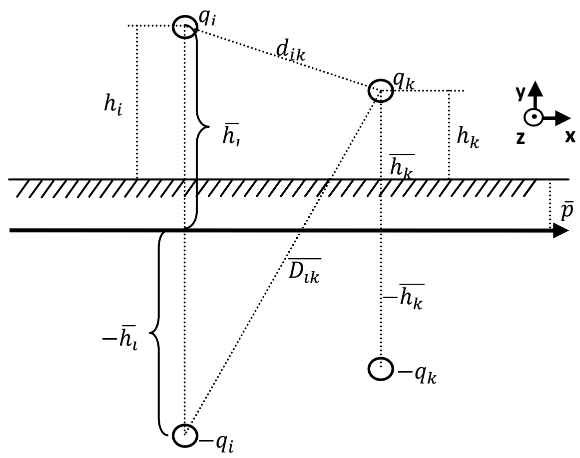

Figure 2 Representation of Dubanton's Method.

For low-frequencies used in this work, the entries of $\boldsymbol{Z_{skin}}$ are defined by

$$\Delta \boldsymbol{Z_{skin}}(\omega) = R_{DC} + j\omega \frac{\mu}{8\pi} \tag{10}$$

where R_{DC} represents the per-unit-length resistance in dc.

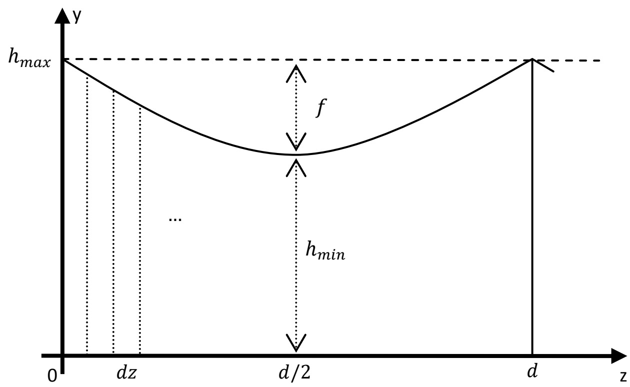

Figure 3 The sag of line conductors between towers along the line span d.

The line conductors are not at the same height between towers, so the entries of $\boldsymbol{L_e}$ and $\boldsymbol{Z_E}$ vary along the coordinate z [BRAND06]. The expression for the conductor's height along z is given by

$$y_k(z) = h_{min} + f\left(\frac{2z_i - d}{d}\right)^2 \tag{11}$$

Where the towers are placed at $z = 0$ and $z = d$, (figure 3).

It's important to underline some aspects:

- Because we are working in quasi-stationary regimes (50Hz) is a decent approach to separate the electric and magnetic field.

-The mitigation loop, if present, should have a length equivalent to a few line spans. The mitigation loop is closed and may include or not a series-capacitor of impedance Z_C. In (5) $\boldsymbol{I}_L$ can be written as

$$\boldsymbol{I}_L = I_L \boldsymbol{S}^T; \boldsymbol{S} = [1 -1] \qquad (12)$$

- The ground wires are traversed by non null time-varying magnetic flux originated by all system currents.

- The currents flowing in a subconductor of a given phase bundle must be different, $I_a \neq I_b$.

Considering the mitigation loop present, with an analyzed line section starting in $z = 0$ and ending in $z = d$, the integration in (2) comes

$$\boldsymbol{V}(l) - \boldsymbol{V}(0) = -\left(\int_{z=0}^{z=l} \overline{\boldsymbol{Z}}'(z)dz\right)\overline{\boldsymbol{I}} \qquad (13)$$

where $\overline{\boldsymbol{I}}$ is pretended to be constant along z. From (13) we have

$$\begin{bmatrix}\Delta\boldsymbol{V}_1\\ \Delta\boldsymbol{V}_2\\ \Delta\boldsymbol{V}_3\\ \Delta\boldsymbol{V}_G\\ \Delta\boldsymbol{V}_L\end{bmatrix} = -\begin{bmatrix}\boldsymbol{Z}_{11}\boldsymbol{Z}_{12}\boldsymbol{Z}_{13}\boldsymbol{Z}_{1G}\boldsymbol{Z}_{1L}\\ \boldsymbol{Z}_{21}\boldsymbol{Z}_{22}\boldsymbol{Z}_{23}\boldsymbol{Z}_{2G}\boldsymbol{Z}_{2L}\\ \boldsymbol{Z}_{31}\boldsymbol{Z}_{32}\boldsymbol{Z}_{33}\boldsymbol{Z}_{3G}\boldsymbol{Z}_{3L}\\ \boldsymbol{Z}_{G1}\boldsymbol{Z}_{G2}\boldsymbol{Z}_{G3}\boldsymbol{Z}_{GG}\boldsymbol{Z}_{GL}\\ \boldsymbol{Z}_{L1}\boldsymbol{Z}_{L2}\boldsymbol{Z}_{L3}\boldsymbol{Z}_{LG}\boldsymbol{Z}_{LL}\end{bmatrix}\begin{bmatrix}\boldsymbol{I}_1\\ \boldsymbol{I}_2\\ \boldsymbol{I}_3\\ \boldsymbol{I}_G\\ \boldsymbol{I}_L\end{bmatrix} = -\begin{bmatrix}\boldsymbol{Z}_{FF}\boldsymbol{Z}_{FG}\boldsymbol{Z}_{FL}\\ \boldsymbol{Z}_{GF}\boldsymbol{Z}_{GG}\boldsymbol{Z}_{GL}\\ \boldsymbol{Z}_{LF}\boldsymbol{Z}_{LG}\boldsymbol{Z}_{LL}\end{bmatrix}\begin{bmatrix}\boldsymbol{I}_F\\ \boldsymbol{I}_G\\ \boldsymbol{I}_L\end{bmatrix} \ (14)$$

The calculation of **Z** is executed using a discretization method, which consists in subdividing the section of the line under analysis into a large number of small segments, each one of length Δl. Considering $l = n_v d$, where n_v is the number of line spans, the matrix **Z** will be written like

$$\boldsymbol{Z} = n_v \sum_{i=1}^{n_s} \boldsymbol{Z}'(z_i)\Delta l \qquad (14)$$

where $z_i = (i-1)\Delta l$, with $i = 1, \ldots, n_s$. The magnetic field produced by each element is computed and added vectorially to the result of all elements.

Having in account that the conductors belonging to a given phase bundle are bonded to each other, and that ground wires are connected to earth (neglecting tower resistances), we can write

$$\begin{cases}\boldsymbol{V}_{ia}(0) = \boldsymbol{V}_{ib}(0)\\ \boldsymbol{V}_{ia}(l) = \boldsymbol{V}_{ib}(l)\\ \Delta\boldsymbol{V}_G = 0\\ \boldsymbol{I}_{ia} + \boldsymbol{I}_{ib} = \boldsymbol{I}_i\end{cases} \qquad (15)$$

In what concerns to the voltage drop in the mitigation loop $\Delta\boldsymbol{V}_L$ (figure 4), we can make

$$\begin{cases}\boldsymbol{V}_{L1}(0) - \boldsymbol{V}_{L2}(0) = -Z_C\boldsymbol{I}\\ \boldsymbol{V}_{L1}(l) = \boldsymbol{V}_{L2}(l)\\ I_{L1} = -I_{L2}\end{cases} \qquad (16)$$

Where Z_C is given by

$$Z_C = jX_s = \frac{1}{j\omega C_s} \qquad (17)$$

Now, we are able to determine all system currents, taking into account the preceding considerations. From (14) we can make

$$\boldsymbol{I}_G = \boldsymbol{Z}_{GG}{}^{-1}(-\boldsymbol{Z}_{GF}\boldsymbol{I}_F - \boldsymbol{Z}_{GL}\boldsymbol{I}_L) \qquad (18)$$

$$\boldsymbol{I}_L = -\underbrace{Y\boldsymbol{S}\boldsymbol{Z}_{LF}\boldsymbol{S}^T}_{\boldsymbol{K}_{LF}}\boldsymbol{I}_F - \underbrace{Y\boldsymbol{S}\boldsymbol{Z}_{LG}\boldsymbol{S}^T}_{\boldsymbol{K}_{LG}}\boldsymbol{I}_G \qquad (19)$$

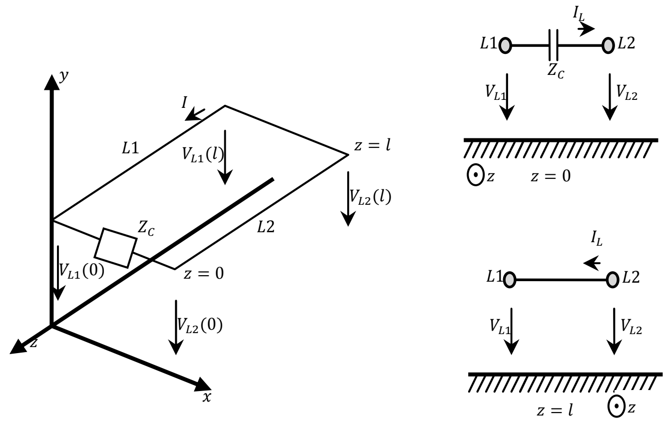

Figure 4 Geometric representation of the near and far ends of the mitigation loop.

where Y is given by

$$Y = \frac{1}{(Z_C + \boldsymbol{S}\boldsymbol{Z}_{LL}\boldsymbol{S}^T)} \qquad (20)$$

Using (18) and (19) we get

$$\boldsymbol{I}_L = -\boldsymbol{\alpha}\boldsymbol{K}_{LF}\boldsymbol{I}_F + \boldsymbol{\alpha}\boldsymbol{K}_{LG}\boldsymbol{Z}_{GG}{}^{-1}\boldsymbol{Z}_{GF}\boldsymbol{I}_F \qquad (21)$$

where

$$\boldsymbol{\alpha} = \left(\boldsymbol{I}_{id} - \boldsymbol{K}_{LG}\boldsymbol{Z}_{GG}{}^{-1}\boldsymbol{Z}_{GL}\right)^{-1} \qquad (22)$$

From (14) we have

$$\Delta\boldsymbol{V}_F = -(\boldsymbol{Z}_{FF}\boldsymbol{I}_F + \boldsymbol{Z}_{FG}\boldsymbol{I}_G + \boldsymbol{Z}_{FL}\boldsymbol{I}_L)$$

Using (18) and (21), we can make

$$\begin{bmatrix}V_{1a}(l) - V_{1a}(0)\\ V_{1b}(l) - V_{1b}(0)\\ V_{2a}(l) - V_{2a}(0)\\ V_{2b}(l) - V_{2b}(0)\\ V_{3a}(l) - V_{3a}(0)\\ V_{3b}(l) - V_{3b}(0)\end{bmatrix} = -[\boldsymbol{Z}_{eq}]\begin{bmatrix}I_{1a}\\ I_{1b}\\ I_{2a}\\ I_{2b}\\ I_{3a}\\ I_{3b}\end{bmatrix} \qquad (23)$$

with

$$\begin{aligned}\boldsymbol{Z}_{eq} = -\boldsymbol{Z}_{FF} + \boldsymbol{Z}_{FG}\boldsymbol{Z}_{GG}{}^{-1}\big(&\boldsymbol{Z}_{GF} - \boldsymbol{Z}_{GL}\boldsymbol{\alpha}\boldsymbol{K}_{LF}\\ &+ \boldsymbol{Z}_{GL}\boldsymbol{\alpha}\boldsymbol{K}_{LG}\boldsymbol{Z}_{GG}{}^{-1}\boldsymbol{Z}_{GF}\big)\\ &+ \boldsymbol{Z}_{FL}\boldsymbol{\alpha}\big(\boldsymbol{K}_{LF} - \boldsymbol{K}_{LG}\boldsymbol{Z}_{GG}{}^{-1}\boldsymbol{Z}_{GF}\big)\end{aligned} \qquad (24)$$

Multiplying (23) by $\boldsymbol{S_1}$, where

$$\boldsymbol{S_1} = \begin{bmatrix}1 & -1 & 0 & 0 & 0 & 0\\ 0 & 0 & 1 & -1 & 0 & 0\\ 0 & 0 & 0 & 0 & 1 & -1\end{bmatrix} \qquad (25)$$

we obtain

$$\begin{bmatrix}0\\0\\0\end{bmatrix}=\begin{bmatrix}Z_{eq11}-Z_{eq21} & Z_{eq12}-Z_{eq22} & Z_{eq13}-Z_{eq23}\\ Z_{eq31}-Z_{eq41} & Z_{eq32}-Z_{eq42} & Z_{eq33}-Z_{eq43}\dots\\ Z_{eq51}-Z_{eq61} & Z_{eq52}-Z_{eq62} & Z_{eq53}-Z_{eq63}\end{bmatrix}$$

$$\begin{matrix}Z_{eq14}-Z_{eq24} & Z_{eq15}-Z_{eq25} & Z_{eq16}-Z_{eq26}\\ \dots Z_{eq34}-Z_{eq44} & Z_{eq35}-Z_{eq45} & Z_{eq36}-Z_{eq46}\\ Z_{eq54}-Z_{eq64} & Z_{eq55}-Z_{eq65} & Z_{eq56}-Z_{eq66}\end{matrix}\Bigg]\begin{bmatrix}I_{1a}\\I_{1b}\\I_{2a}\\I_{2b}\\I_{3a}\\I_{3b}\end{bmatrix} \quad (26)$$

We are thus with a system of 3 equations and 6 variables. However using the fourth equation of (15) we can reach three additional equations and using Matlab we can solve the system, determining all the currents on the power line system,

$$\begin{cases}I_{1a}+I_{1b}=I_1\\ I_{2a}+I_{2b}=I_2\\ I_{3a}+I_{3b}=I_3\end{cases}$$

With all the currents known we could advance to magnetic field calculation. The complex amplitude of the magnetic induction field, $\overline{\boldsymbol{B}}$ in the space surrounding the overhead line is given by

$$\overline{\boldsymbol{B}}=\overline{\boldsymbol{B}}_F+\overline{\boldsymbol{B}}_G+\overline{\boldsymbol{B}}_L \quad (27)$$

where $\overline{\boldsymbol{B}}_F$ refer to the phase conductors, $\overline{\boldsymbol{B}}_G$ refer to the ground wires and $\overline{\boldsymbol{B}}_L$ to the mitigation loop.

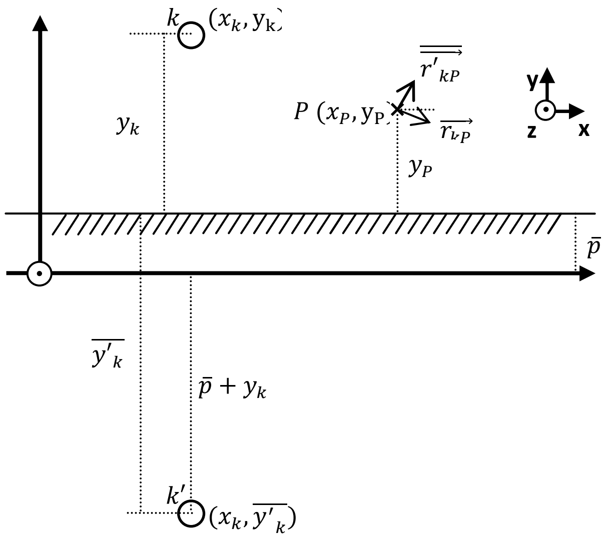

Figure 5 Specification of the coordinates required to magnetic field calculation produced by conductor k in point P.

In figure 5 are illustrated the magnetic field calculation in point P, originated by a generic conductor, where

$$\overrightarrow{r_{kP}}=(x_P-x_k)\vec{u}_x+(y_P-y_k)\vec{u}_y \quad (28)$$

$$\overrightarrow{r'_{kP}}=(x_P-x_k)\vec{u}_x+\left(y_P-\overline{y'_k}\right)\vec{u}_y \quad (29)$$

$$\overline{y'_k}=-y_k-2\bar{p} \quad (30)$$

Thus, currents in conductors k and k' (image of k), will contribute to magnetic field in point P through

$$\overline{\overline{\boldsymbol{H}}}_{kP}=\left[-\frac{y_P-y_k}{2\pi\, r_{kP}{}^2}\overline{\boldsymbol{I}}_k+\frac{y_P-\overline{y'_k}}{2\pi\overline{r'_{kP}}^2}\overline{\boldsymbol{I}}_k\right]\vec{u}_x+\left[\frac{x_P-x_k}{2\pi\, r_{kP}{}^2}\overline{\boldsymbol{I}}_k-\frac{x_P-x_k}{2\pi\overline{r'_{kP}}^2}\overline{\boldsymbol{I}}_k\right]\vec{u}_y \quad (31)$$

For comparison purposes it's important the calculation of the rms value of the field. For n_c conductors, we have

$$H_{rms}=\sqrt{\left(\sum_{k=1}^{n_c}H_{kxr}\right)^2+\left(\sum_{k=1}^{n_c}H_{kxi}\right)^2+\left(\sum_{k=1}^{n_c}H_{kyr}\right)^2+\left(\sum_{k=1}^{n_c}H_{kyi}\right)^2} \quad (32)$$

III. ELECTRIC FIELD EVALUATION

For the electric field evaluation, the adopted procedure is similar to the magnetic field calculation. However, because the magnetic field evaluation was the main subject of this paper, in the electric field analysis, a simpler approach has been made. The phase bundle conductors were considered to be at the average height above ground. The charges q in conductors are determined from the voltages and Maxwell potential coefficients [GEC82]

$$\boldsymbol{q}=\boldsymbol{P}^{-1}\boldsymbol{V} \quad (32)$$

where

$$\boldsymbol{P}^{-1}=\boldsymbol{C} \quad (33)$$

and $\boldsymbol{q}$ is the charges vector. $\boldsymbol{V}$ is the column vector of the line voltages. The phase voltages are specified, however, voltages in the remaining conductors, are unknown (except on ground wires, $\Delta\boldsymbol{V}_G=0$). In (32), we have

$$\begin{bmatrix}\boldsymbol{q}_1\\\boldsymbol{q}_2\\\boldsymbol{q}_3\\\boldsymbol{q}_G\\\boldsymbol{q}_L\end{bmatrix}=\begin{bmatrix}\boldsymbol{C}_{11}\boldsymbol{C}_{12}\boldsymbol{C}_{13}\boldsymbol{C}_{1G}\boldsymbol{C}_{1L}\\\boldsymbol{C}_{21}\boldsymbol{C}_{22}\boldsymbol{C}_{23}\boldsymbol{C}_{2G}\boldsymbol{C}_{2L}\\\boldsymbol{C}_{31}\boldsymbol{C}_{32}\boldsymbol{C}_{33}\boldsymbol{C}_{3G}\boldsymbol{C}_{3L}\\\boldsymbol{C}_{G1}\boldsymbol{C}_{G2}\boldsymbol{C}_{G3}\boldsymbol{C}_{GG}\boldsymbol{C}_{GL}\\\boldsymbol{C}_{L1}\boldsymbol{C}_{L2}\boldsymbol{C}_{L3}\boldsymbol{C}_{LG}\boldsymbol{C}_{LL}\end{bmatrix}\begin{bmatrix}\boldsymbol{V}_1\\\boldsymbol{V}_2\\\boldsymbol{V}_3\\\boldsymbol{V}_G\\\boldsymbol{V}_L\end{bmatrix}=\begin{bmatrix}\boldsymbol{C}_{FF}\boldsymbol{C}_{FG}\boldsymbol{C}_{FL}\\\boldsymbol{C}_{GF}\boldsymbol{C}_{GG}\boldsymbol{C}_{GL}\\\boldsymbol{C}_{LF}\boldsymbol{C}_{LG}\boldsymbol{C}_{LL}\end{bmatrix}\begin{bmatrix}\boldsymbol{V}_F\\\boldsymbol{V}_G\\\boldsymbol{V}_L\end{bmatrix} \quad (34)$$

Considering the last equation of (34) we have

$$[1\ \ 1]\begin{bmatrix}\boldsymbol{q}_{L1}\\\boldsymbol{q}_{L2}\end{bmatrix}=[1\ \ 1][\boldsymbol{C}_{LF}][\boldsymbol{V}_F]+[1\ \ 1][\boldsymbol{C}_{LL}]\left(\begin{bmatrix}0\\Z_CI_L\end{bmatrix}+\begin{bmatrix}1\\1\end{bmatrix}\boldsymbol{V}_{L1}\right) \quad (35)$$

$$\boldsymbol{V}_{L1}=-[1\ \ 1][\boldsymbol{C}_{LL}]\begin{bmatrix}1\\1\end{bmatrix}^{-1}\left([1\ \ 1][\boldsymbol{C}_{LF}][\boldsymbol{V}_F]+[1\ \ 1][\boldsymbol{C}_{LL}]\begin{bmatrix}0\\Z_CI_L\end{bmatrix}\right) \quad (36)$$

At this point, we know all the voltages in the system. Thus, the electric field in the point P, produced by the charges in k and k' (figure 6) is given by:

$$\overline{\overline{\boldsymbol{E}}}_{kP}=\frac{\overline{\boldsymbol{q}_k}}{2\pi\,\varepsilon_0 r_{kP}}\vec{u}_k-\frac{\overline{\boldsymbol{q}_k}}{2\pi\,\varepsilon_0 r_{k'P}}\vec{u}_{k'} \quad (37)$$

where $r_{k'P}$ is given by:

$$r_{k'P}=\sqrt{(x_P-x_k)+(y_P-y'_k)} \quad (38)$$

In (37), we have

$$\vec{\overline{E}}_{kP} = \frac{\overline{q_k}}{2\pi\varepsilon_0}\left[\frac{x_P-x_k}{r_{kP}^2} - \frac{x_P-x_{k'}}{r_{k'P}^2}\right]\vec{u}_x + \frac{\overline{q_k}}{2\pi\varepsilon_0}\left[\frac{y_P-y_k}{r_{kP}^2} - \frac{y_P-y_{k'}}{r_{k'P}^2}\right]\vec{u}_y \quad (39)$$

For n_c conductors, the rms value of electric field is given by

$$E_{rms} = \\ = \sqrt{\left(\sum_{k=1}^{n_c} E_{kxr}\right)^2 + \left(\sum_{k=1}^{n_c} E_{kxi}\right)^2 + \left(\sum_{k=1}^{n_c} E_{kyr}\right)^2 + \left(\sum_{k=1}^{n_c} E_{kyi}\right)^2} \quad (34)$$

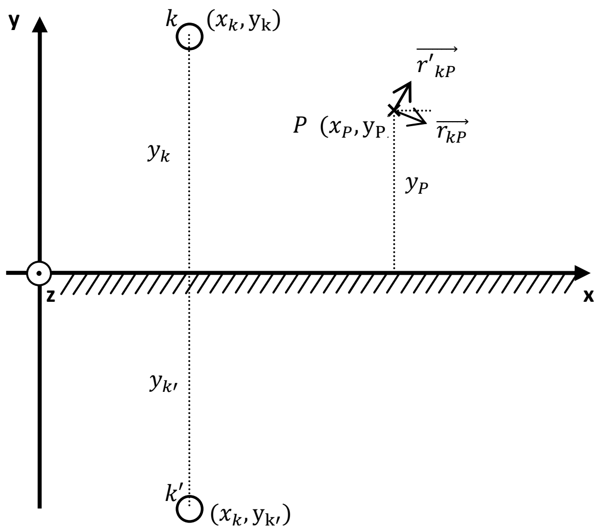

Figure 6 Specification of the coordinates required to magnetic field calculation produced by conductor k in point P.

IV. SIMULATION RESULTS

<u>Magnetic Field:</u>

Here we are going to apply the theory developed previously to a single-circuit power line. For the single-circuit power line with flat configuration table I summarizes conductor characteristics.

Cond. Nr.	Dia-meter (mm)	X Coord. at tower (m)	Y Coord. at tower (m)	Sag (m)	Rdc 20ºC (mΩ/ km)
1-a	31.8	-12.2	26	12	57.3
1-b	31.8	-11.8	26	12	57.3
2-a	31.8	-0.2	26	12	57.3
2-b	31.8	0.2	26	12	57.3
3-a	31.8	11.8	26	12	57.3
3-b	31.8	12.2	26	12	57.3
G1	14.6	-8	36	9	372
G2	14.6	8	36	9	372
L1	22.4	-12	16	9	131
L2	22.4	12	16	9	131

Table 1 *Characteristics of line conductors.*

A soil with a resistivity ρ of 100 Ωm has been considered for this simulation. The distance between consecutive towers is $d = 300m$. The mitigation loop considered (if exists) has the length of three line spans. For a 400kV, $S = 1400\ MVA$, the phase-conductor currents $\mathbf{I_P}$ are defined by a set of 50Hz sinusoidal currents, with 2kA rms:

$$\mathbf{I_P} = \begin{bmatrix} I_1 \\ I_2 \\ I_3 \end{bmatrix} = \sqrt{2}.2 \begin{bmatrix} 1 \\ e^{-\frac{2\pi}{3}} \\ e^{+\frac{j2\pi}{3}} \end{bmatrix} kA \quad (35)$$

For comparison purposes, considering that the mitigation loop is absent, at an observation point P of coordinates $x_P = 0$ and $y_P = 1.8m$, the rms value of the magnetic induction vector is

$$B_{std} = 32.16\ \mu T \quad (36)$$

Introducing the mitigation loop, table 2 summarizes the results concerning the complex amplitudes of all conductor currents. Two situations were considered. First, the mitigation loop is absent; second, the mitigation loop is present and short-circuited.

Conductor	*Without mitigation loop*	*With short-circuited mitigation loop*
1a	994.3 - j5.6	994.8 - j5.6
1b	1005.7 + j5.6	1005.2 + j5.6
2a	-515.1 - j861.6	-513.6 – j 861.7
2b	-484.9 - j870.4	-486.4 - j870.4
3a	-502 + j873.8	-501.5 + j873.7
3b	-498 + j858.3	-498.5 + j858.3
G1	-104.7 + j6.9	-97.3 + j9.7
G2	108.5 + j31.9	101.1 + j29.1
L1	0	-232.4 + j65.8
L2	0	232.4 – j65.8

Table 2 Complex amplitudes of conductor currents with and without mitigation loop.

With a short-circuited mitigation loop we obtain

$$B_{rms} = 26.73\ \mu T = 0.83\ B_{std} \quad (37)$$

The result in (37) shows the real effectiveness of the mitigation loop. The presence of the loop reduces the field in 17% in the observation point (figure 7).

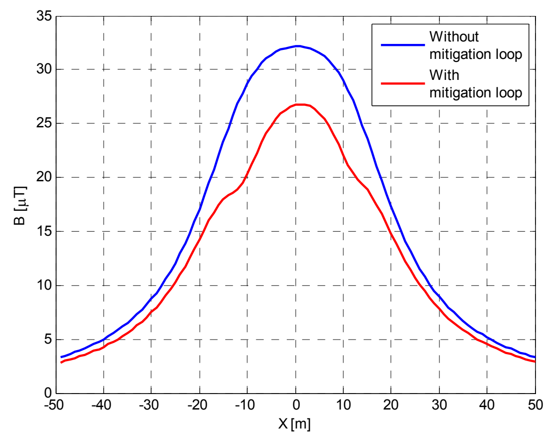

Figura 7 Representation of magnetic field variation with the coordinate x, for the two situations presented previously (mid-span).

Varying the distance of the mitigation loop conductors to the center of the tower (x=0), we obtained figure 8.

The minimum value of the field is obtained for the locations $x_{L1} = -10$ e $x_{L2} = 10m$. From now on, we will work with those locations for the mitigation loop conductors. To improve the results we will insert an appropriately chosen series-capacitor in the loop [BRAND06]. Figure 9 shows the best and worst capacitances of the capacitor to be inserted. For the optimal situation we have

$$X_s = -0.501\Omega;\ C_s = 6.35mF; B_{rms} = 23.67\mu T = 0.74B_{std} \quad (38)$$

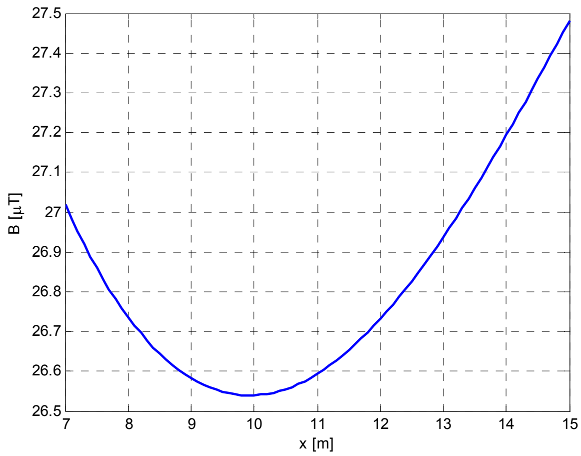

Figure 8 Representation of magnetic field B variation with the position through coordinate x.

The worst situation is characterized by

$$X_s = -1.023\Omega;\ C_s = 3.11mF; B_{rms} = 47.19\mu T = 1.46B_{std} \quad (39)$$

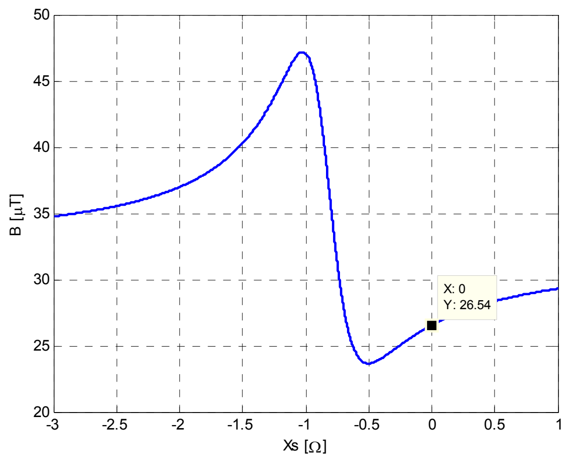

Figure 9 Magnetic induction field as function of the reactance X_s of the compensation capacitor inserted in the mitigation loop.

The capacitor compensation scheme does not seem to be an outstanding solution. The reduction in the field is weak and the cost would be high due to the elevated capacitance required. On the other hand a mistake on the choice of capacitance could lead to an increase in the B field.

Cond.	$C_s = 6.35mF$	$C_s = 3.11mF$	***Short Circuited***
1a	994.6 - j5.5	994.2 - j5.2	994.5 - j5.6
1b	1005.4 + j5.5	1005.8 + j5.2	1005.5 + j5.6
2a	-512.1 - j860.8	-516.4 - j856.9	-513.6 – j 861.7
2b	-487.9 - j871.3	-483.6 - j875.1	-486.4 - j870.4
3a	-501.7 + j873.8	-502.1 + j874.1	-501.8 + j873.8
3b	-498.3 + j858.2	-497.9 + j857.9	-498.2 + j858.3
G1	-94.1 + j15.3	-117.9 + j23.7	-98.6 + j9.3
G2	97.9 + j23.5	121.7 + j15.1	102.4 + j29.5
L1	-458.1-j13.9	19.6-j724.9	-215.5 + j59.7
L2	458.1+j13.9	-19.6+j724.9	215.5 - j59.7

Table 3 Complex amplitudes of conductor currents with compensation capacitor

In table 3 are shown the complex amplitudes of the system currents, considering the two schemes using compensation capacitor. Figure 10 shows the field variation for the three situations analyzed: line without mitigation; with short-circuited mitigation loop; and with the optimal series capacitor. The option with series capacitor experiments bigger variations on the B field for short distances in space.

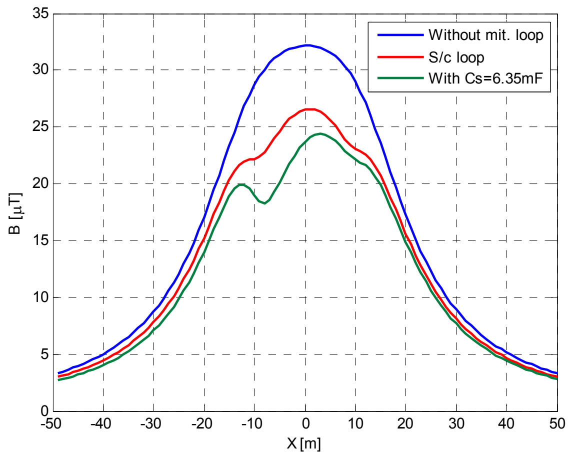

Figure 10 Representation of B field variation with the distance in the coordinate x, for the three situations analyzed previously (mid-span).

<u>Electric field:</u>

Using the calculation method described above, for the same single circuit line configuration we are going to analyze the electric field variation. For the standard case (the same used for magnetic field calculation) we obtain

$$E = 0.65\ kV/m \quad (40)$$

The result is in a high degree below the ICNIRP limits [ICNIRP98]. However, in contrast of magnetic field, the maximum value of electric field doesn't occur in the centre of the line. It occurs near the edge of right-of-way (figure 11).

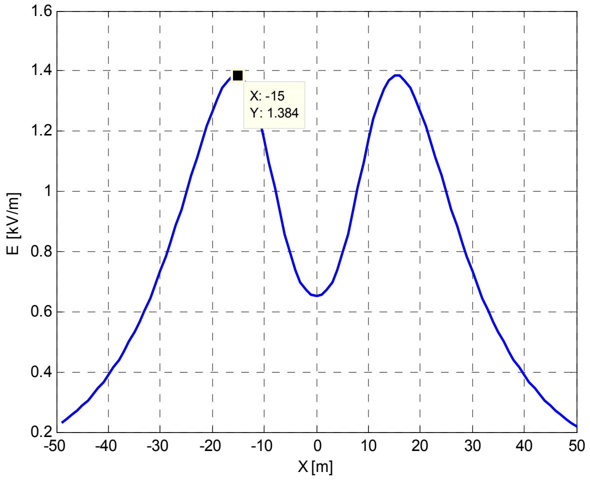

Figure 11 Representation of electric field variation with the coordinate x

The maximum value is verified for $x = -15m$ and $x = 15m$, where we obtain

$$E = 1.38\ kV/m \tag{41}$$

Using the flat line geometry in figure 1, ignoring ground wires, we change the distance between conductors and check the effects in the electric field. Considering D_c the distance between phases (figure 12), in figure 13 the variation of E field is presented.

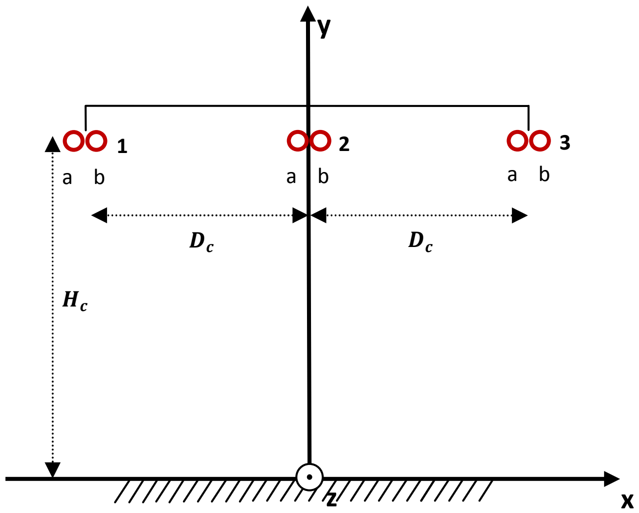

Figure 12 Illustration of distances D_c and H_c in flat configuration.

Decreasing the distance between phase conductors, the electric field produced by the line also decrease. In figure 14 is presented the variation of the electric field varying conductor's height H_c to the ground. Bigger heights produce lower fields, as expected.

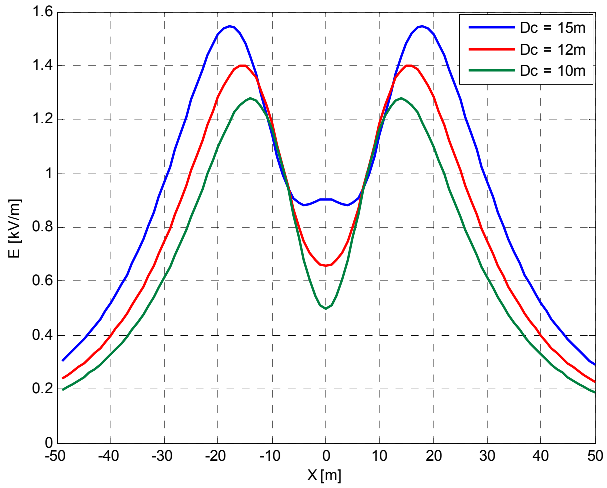

Figure 13 Representation of the electric field variation for different distances between phase conductors.

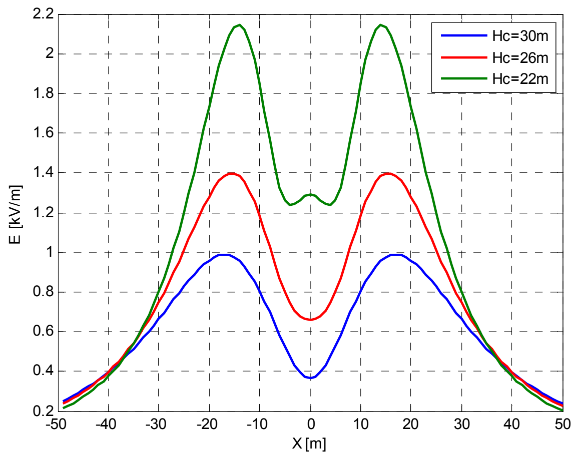

Figure 14 Representation of the electric field variation for different heights to the ground.

V. CONCLUSIONS

In this paper was developed a general model for the computation of magnetic and electric fields. A bigger attention was given to the magnetic field, because it's an object of bigger concerns by the scientific community. The model takes into account a large variety of effects allowing a rigorous evaluation of magnetic field. That includes the partition of bundle-phase conductors into subconductors, includes ground wires effects and includes the contribution of the sag effect on line conductor. A numerical and graphical result concerning the evaluation of the fields was obtained. The mitigation loop technique with and without compensation capacitor was analyzed in detail. The effectiveness of this solution was discussed. For future works other magnetic field reduction techniques can be explored. In what concerns to the electric field evaluation, a more detailed approach is suggested as a project to be addressed in the future.

REFERENCES

[CARST95] E. L. Carstensen, “Magnetic fields and câncer” *IEEE Eng. Biol.,* pp. 362-369, Jul./Aug. 1995.

[ICNIRP98] International Commission of Non Ionizing Radiation Protection (ICNIRP), “Guidelines for limiting exposure to time-varying electric, magnetic and electromagnetic fields (up to 300Ghz)”, *Health Phys.,* vol.74, no.4, pp. 494-522, Apr. 1998.

[WASHI92] Electric Transmission Research Needs Task Force, “Electric and Magnetic Field Reduction: Research Needs”, *Report prepared for the State of Washington, USA,* Jan. 1992.

[SHPER96] A. B. Shperling, L. Menemenlis-Hopkins, B. Fardanesh, B. Clairmont, and D. Childs, “Reduction of Magnetic Fields from Transmission Lines using Passive Loops”, *CIGRE International Conference,* Report 36-103, Paris, 1996.

[CELO02] S. Celozzi, “Active compensaton and partial shields for the power-frequency magnetic field reduction”, in *2002 Int. Symp. Electromagnetic Compatibility*, vol.1, pp. 222-226, 2002.

[MEMAR05] A. R. Memari, “Optimal Calculation of Impedance of na Auxiliary Loop to Mitigate Magnetic Field of a Transmission Line”, *IEEE Trans. On Power Del.,* vol.20, no.2, April 2005.

[WALL93] R.A. Walling, J. J. Paserba, C.W. Burns, “Series-Capacitor compensated shield scheme for enhanced mitigation of transmission lines magnetic fields”, *IEEE Trans. Power Del.*, vol.8, no.1, pp. 461-468, Jan. 1993.

[DUBAN69] C. Dubanton, “Calcul approché des parametres primaires et secondaires d’une ligne de transport”, *EDF Bulletin de la Direction des etudes et Recherches,* no. 1, pp. 53-62, 1969.